Journal of Thermal Analysis and Calorimetry (2018) 133:673–682
https://doi.org/10.1007/s10973-018-7178-y

Molecular simulation and experimental study on thermal decomposition of *N*,*N*′-dinitrosopentamethylenetetramine

Yi Liu[1,2] · Yu Wang[3] · Chi-Min Shu[4] · Dongfeng Zhao[2,3] · Wanghua Chen[5] · Jun Zhang[5]

Received: 7 September 2017 / Accepted: 6 March 2018 / Published online: 12 March 2018

Abstract

N,*N*′-dinitrosopentamethylenetetramine (DNPT), which is a widely used as blowing agent in the rubber industry, tends to be unstable when affected by high temperature and specific impurities. The runaway of DNPT has caused several accidents and led to enormous economic losses in the world. We determined its thermal hazard properties and decomposition paths for process safety. Characteristic parameters of pure and impure (added with water and nitric acid) DNPT were obtained under different heating rates by differential scanning calorimetry experiments. Those parameters were used to calculate the apparent activation energy with the Kissinger method. Thermogravimetry was used to obtain exothermic onset temperature and peak temperature under different heating rates. The apparent activation energy of DNPT decomposition reaction was achieved by model-free kinetics approach. Quantum mechanics model was used to explore the thermal decomposition reaction pathways of DNPT. DFT B3LYP density functional method, and the 6-311++G (D) basis set was selected for molecular simulation by Gaussian 09 software. The single point energy, zero-point energy, thermal energy, thermal enthalpy, and thermal free energy were acquired. The bond dissociation energy (BDE) at different excited states was calculated. By comparing BDE of different excited states, the thermal decomposition reaction pathways can be predicted. The results of experiments and simulations can be applied as safety guidance to deal with DNPT's loss prevention during transportation, handling, and storage, even emergency response.

Keywords Characteristic parameters · Model-free kinetics · Quantum mechanics model · Bond dissociation energy · Thermal decomposition reaction pathway

List of symbols

E_a	Apparent activation energy, kJ mol^{-1}
E_0	Total energy of free radicals or molecules at 0 K, kJ mol^{-1}
m_{DNPT}	DNPT sample mass, mg
mH_2O	Mass of the added water, mg
m_{HNO3}	Mass of the added nitric acid solution, mg
r^2	Correlation coefficient, dimensionless
T	Thermodynamics temperature, °C
T_0	Exothermic onset temperature, °C
T_m	Maximum reaction temperature, °C
T_{end}	End temperature of reaction, °C
ΔE	Single point energy variation, kJ mol^{-1}
$\Delta E'$	Zero-point energy variation, kJ mol^{-1}
ΔH_d	Heat of decomposing, J g^{-1}
ΔZPE	Difference between the total zero point of free radicals or molecules after dissociation and the zero energy before dissociation, kJ mol^{-1}
α	Conversion degree, dimensionless
β	Heating rate, °C min^{-1}

✉ Yi Liu
liuyi@upc.edu.cn

1 State Key Laboratory of Heavy Oil Processing, China University of Petroleum (East China), Qingdao 266580, China

2 College of Chemical Engineering, China University of Petroleum (East China), Qingdao 266580, China

3 Center for Safety, Environmental, and Energy Conservation Technology, China University of Petroleum (East China), Qingdao 266580, China

4 Department of Safety, Health, and Environmental Engineering, National Yunlin University of Science and Technology, Yunlin 64002, Taiwan, ROC

5 Department of Safety Engineering, School of Chemical Engineering, Nanjing University of Science and Technology, Nanjing 210094, China

Introduction

N,*N*′-dinitrosopentamethylenetetramine (DNPT) is a type of sensitive nitrite organic compound. As an organic blowing agent, it is widely used in some industries, such as emulsion explosive, rubber, plastics, and three-dimensional printing. DNPT has the advantage of large gas volume, high foaming efficiency, no color change, no pollution, and low price [1, 2]. Documentation of worldwide explosions and fires caused by DNPT in the past decades is given in Table 1. The DNPT spontaneous combustion at Japan Kobe Port is attributed to the thermal accumulation in the container under continuous sunlight and impurity incorporation [3]. Partial overheating caused by thermal accumulation is the dominant reason for three DNPT accidents in China [4–6]. These DNPT accidents resulted in 18 deaths and 25 injuries, as well as enormous property damages.

3,7-Dinitro-l,3,5,7-tetra-azabicyclo[3.3.l]non (DPT) has a similar structure to DNPT. Radhakrishnan et al. [7] studied the thermal decomposition properties and the decomposition products of DPT. The effects of nitric acid (HNO_3), ammonium ion, and ammonium nitrate on the thermal decomposition of DPT and its influence mechanism were also studied [8, 9, 13]. Due to its extensive use and thermal risk, numerous studies on the properties of DNPT have been presented. The effect of rubber on thermal decomposition of DNPT has been extensively investigated. The decomposition characteristics of DNPT in different rubber media and different types of rubber media are entirely different [10–17]. The thermal decomposition reaction process of DNPT has also been predicted [18], but has not yet been verified by experiments and simulations. The active sequence of each nitrogen atom in DNPT during the decomposition process has been obtained by theoretical simulation of the charge of nitrogen atom [13]. The reaction mechanism of DNPT under the influence of ammonium nitrate has been explored, but the effects of carbon atoms have been neglected during the simulation process. Tall et al. [19] delved into the degree of filling up of the volume for thermal decomposition of DNPT. Their results showed that the value of decomposition heat strongly depends on the degree of filling up of the volume.

Previous studies on DNPT focused on the applications of the foaming agent. Few of them considered the transportation and storage of DNPT from the loss prevention point of view. Studies pertaining to DNPT, effects of impurities for DNPT, and analysis of DNPT's decomposition reaction mechanism are insufficient. We studied thermal hazard and thermal decomposition mechanism of DNPT by combining experiments with molecular simulations. The aim was to promote an understanding of thermal hazard of DNPT and provide more theoretical bases for prevention and control of fire and explosion in the process of producing, transporting, storing and using, and even emergency disposal.

Table 1 Selected fires and explosions caused by thermal runaway of DNPT

Year	Country	Sector	Deaths/injuries
1979	Japan	Transportation	0/0
2008	China	Storage	0/15
2009	China	Transportation	18/10
2013	China	Production	0/0

Experiment and simulation

Differential scanning calorimetry experiment

The DSC in this article was produced by Beijing Henven Scientific Instrument Co., Ltd. (Beijing, China) whose type was HSC-1/2. The sample in the DSC experiment was light yellow powdery DNPT with a purity of 98 mass%, which was produced by Shandong Western Asia Chemical Industry Co., Ltd. (Shandong Province, China) in Western Shandong Province and dried at 45 °C for 1 h prior to the experiment. The heating rates of pure DNPT experiment were 2.0, 4.0, 6.0, 8.0, 10.0, and 12.0 °C min^{-1}. The heating rates of the experiment were 2.0, 4.0, 6.0, and 10.0 °C min^{-1} when distilled water or acid solution was added in DNPT. The acid solution was diluted by HNO_3 with a purity of 65–68 mass%. The initial temperature was room temperature, and the termination temperature was 350 °C. The sample loading was 5.0 ± 0.1 mg per run, and the process of the reaction was in the air atmosphere.

Thermogravimetry–infrared experiment

We used a combined instrument of thermogravimetry (Q500, TA Corp., USA) and infrared (Nicolet 6700, Thermo Scientific, USA). The sample was the same as the DSC experiment, and the heating rates of the TG experiment were 1.0, 3.0, and 5.0 °C min^{-1}. The initial temperature was room temperature, and the termination temperature was 350 °C. The sample loading was 20.0 ± 1.0 mg per run, the process of the reaction was in the dynamic atmosphere of nitrogen, and gas flow rate was 50.0 mL min^{-1}. The infrared spectra of the products were measured when the mass loss rate was the highest at different heating rates.

Molecular simulation

To delve into the thermal decomposition path of DNPT, Gaussian 09 and Gauss View 5.0 were adopted to optimize and calculate the energy of free radicals of DNPT molecules and their bond dissociations in the pyrolysis process by the density functional method (DFT-B3LYP) and the 6-311++G (D) basis set.

Results and discussion

Figure 1 shows heat flow versus temperature curve by DSC experiments for 98 mass% DNPT under various β. According to Fig. 1 and Table 2, T_0 slightly fluctuated at approximately 200 °C with the increase in β. The exothermic onset temperature of DNPT was almost unaffected by β. T_m and T_{end} tended to increase with the increase in β. With the growth of β, ΔH_d showed a decreasing trend.

Figures 2 and 3 illustrate the heat flow versus temperature curve of DNPT with various water content under different heating rates. Two peaks are shown in both Figs. 2 and 3. The first endothermic peak was formed by the endothermic vaporization of the water in the crucible. The second peak was the exothermic peak, which was the exothermic reaction peak of DNPT. Table 3 showes the change in T_0 was relatively small with the increase in the heating rate. The heating rate hardly affected the apparent onset reaction temperature of DNPT, when water was added. T_m and T_{end} both tended to increase with the increase in β. With the increase in the heating rate, ΔH_d showed decreasing tendency.

Table 2 Characteristic parameters for thermal decomposition of pure DNPT by DSC

β/°C min^{-1}	m/mg	T_0/°C	T_m/°C	T_{end}/°C	$-\Delta H_d$/J g^{-1}
2.0	5.1	198.6	201.5	202.4	1.45
4.0	4.9	202.6	206.9	208.6	1.23
6.0	5.0	200.0	206.8	208.5	1.10
8.0	5.1	201.6	208.1	212.7	1.02
10.0	5.1	200.3	209.9	214.9	0.98
12.0	5.0	200.9	210.6	216.9	0.95

According to Fig. 4 and Table 4, T_0, T_m, T_{end}, and ΔH_d increased when more water was added. As for thermal safety, water can improve the exothermic onset temperature of DNPT. From the perspective of energy, the apparent activation energy of DNPT reaction also rose sharply when more water was added. As listed in Table 5, the apparent activation energy increased with the amount of water. Higher activation energies render a higher sensitivity toward temperature variation. An extremely very slow reaction at low temperatures may become fast and therefore dangerous at higher temperatures [20]. However, T_m, T_{end}, and ΔH_d also increased when more water was added, revealing the reaction was faster and more dangerous. Therefore, keeping DNPT and the environment dry was beneficial to the transportation and storage safety of DNPT. In view of emergency preparedness and response, using water is improper to lessen the risk of thermal runaway of DNPT.

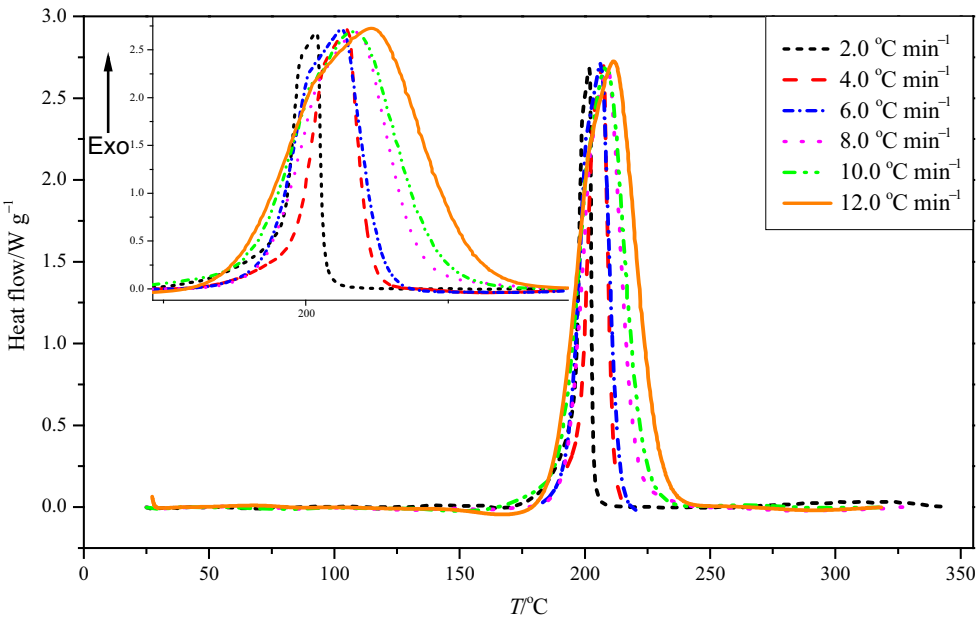

Fig. 1 Heat flow versus temperature curve of pure DNPT by DSC

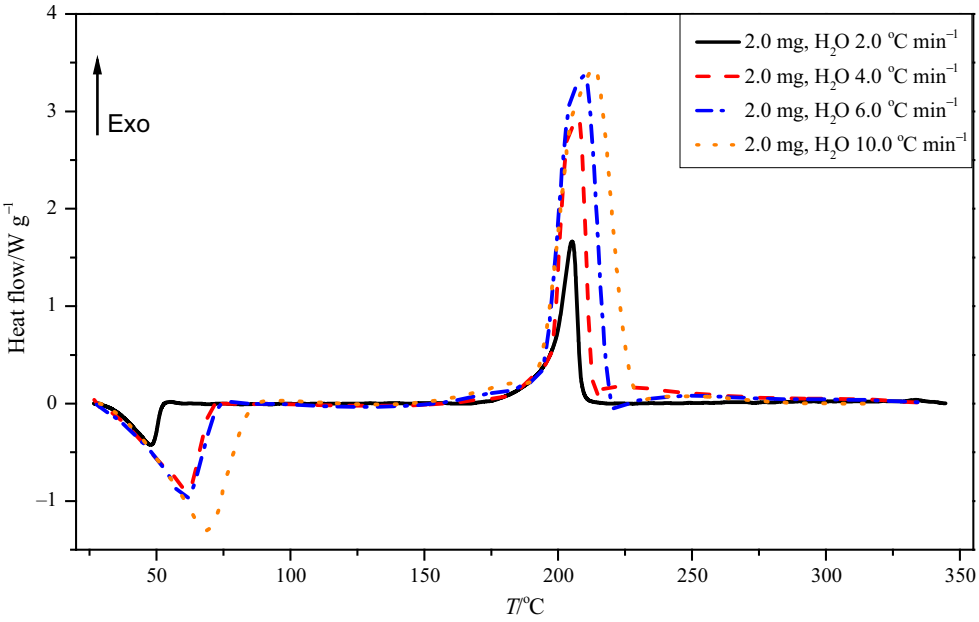

Fig. 2 Heat flow versus temperature curve of DNPT with 2.0 mg H_2O by DSC

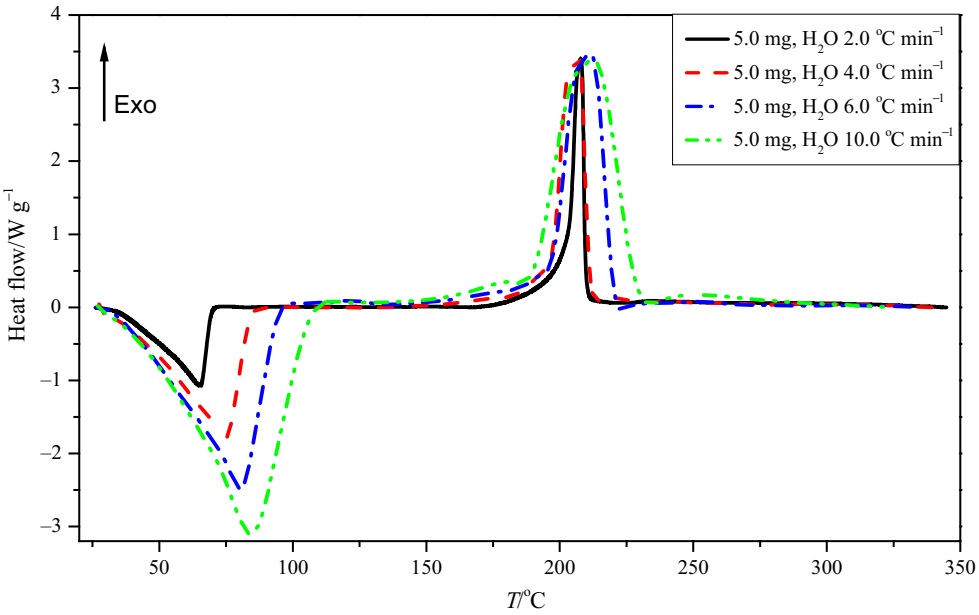

Fig. 3 Heat flow versus temperature curve of DNPT with 5.0 mg H_2O by DSC

Table 3 Characteristic parameters for thermal decomposition of DNPT with H_2O by DSC

β/°C min^{-1}	m_{DNPT}/mg	mH_2O/mg	T_0/°C	T_m/°C	T_{end}/°C	$-\Delta H_d$/J g^{-1}
2.0	5.0	2.0	198.2	205.5	208.0	1.49
4.0	5.0	2.0	203.0	207.5	209.0	1.35
6.0	4.9	2.0	203.4	209.9	212.5	1.32
10.0	5.0	2.0	204.2	212.9	217.6	1.11
2.0	5.1	5.0	205.8	207.6	209.0	1.88
4.0	5.1	5.0	202.2	209.5	208.6	1.49
6.0	5.1	5.0	205.4	210.7	214.8	1.46
10.0	4.9	5.0	203.7	212.3	217.6	1.24

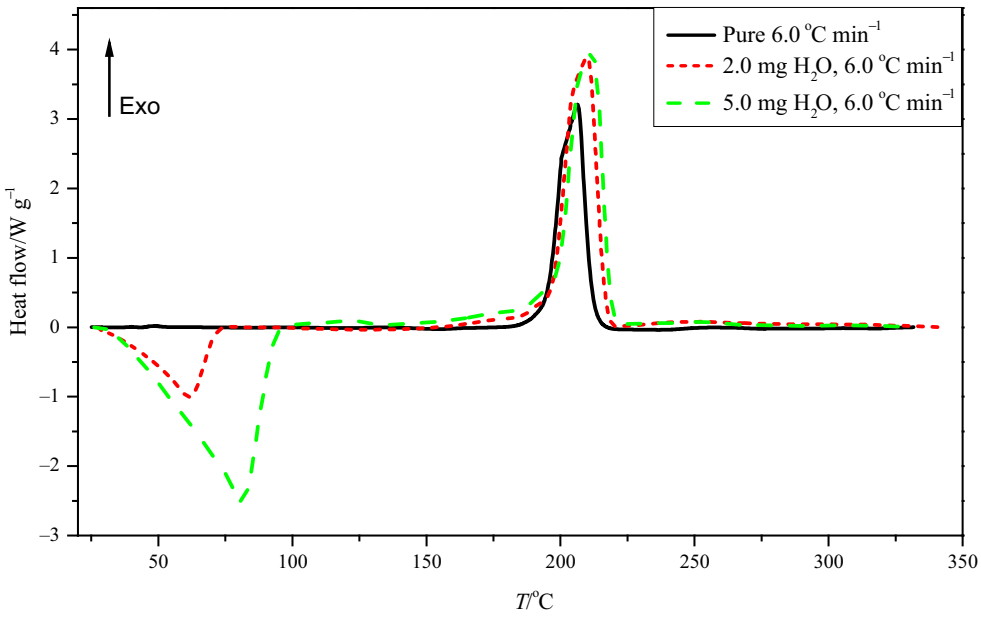

Fig. 4 Heat flow versus temperature curve of DNPT with different mass of water by DSC

Table 4 Characteristic parameters for thermal decomposition of DNPT with various mass of H_2O by DSC

β/°C min^{-1}	m/mg	m_{H_2O}/mg	T_0/°C	T_m/°C	T_{end}/°C	$-\Delta H_d$/J g^{-1}
6.0	5.0	–	200.0	206.8	208.5	1.10
6.0	4.9	2.0	203.4	209.9	212.5	1.32
6.0	5.1	5.0	205.4	212.0	214.8	1.46

Table 5 Apparent activation energy of DNPT with various mass of water by Kissinger method

No.	Samples	E_a/kJ mol^{-1}	r^2
1	DNPT	160.83	0.9341
2	DNPT + 2.0 mg H_2O	172.80	0.9678
3	DNPT + 5.0 mg H_2O	285.30	0.9990

During production, transportation, and storage process of DNPT, not only could water be mixed, but dilute acid which was the most common acid in the production environment of DNPT could also be mixed. Therefore, dilute nitric acid was used as an acid impurity. Adding HNO_3 of different pH values to the DNPT sample was used to compare the effect of acid concentration on the thermal stability of DNPT. As shown in Fig. 5 and Table 6, T_0, T_m, and T_{end} of DNPT decreased first and then increased following the increase in the pH. Inorganic acids contributed to the reaction of DNPT, but H_2O of the acid solution can also affect the reaction. The effect of acid on the reaction was stronger than that of water when the pH was less than or equal to 1. When pH was larger than or equal to 3, H_2O in the solution became the decisive factor affecting the reaction.

The DSC experiment was carried out in air atmosphere, but not all DNPT could contact with the air due to the large amount of DNPT in the transportation and storage processes. To further study the thermal decomposition properties of DNPT, the TG-IR experiment under inert atmosphere was employed.

Figure 6 shows the analysis curves of TG and DTG, in which both consisted of two stages. The first stage was near 100 °C, and DNPT lost about 5 mass% in this stage. DNPT lost approximately 90 mass% in the second stage, which was near 200 °C. According to the temperature range and percentage of loss of mass, the first stage was the process of dehydration and the second stage was the process of thermal decomposition. The characteristic parameters of thermal decomposition are given in Table 7. The greater the heating rate was, the more visible the temperature hysteresis was.

According to the Friedman method, the apparent activation energy of DNPT can be obtained by model-free kinetics. Figure 7 gives the apparent activation energy and the correlation coefficient. The apparent activation energy also fluctuated with respect to α value. The first peak of the apparent activation energy curve was the apparent activation energy of the initial reaction of DNPT, and the apparent activation energy was 165.4 kJ mol^{-1}.

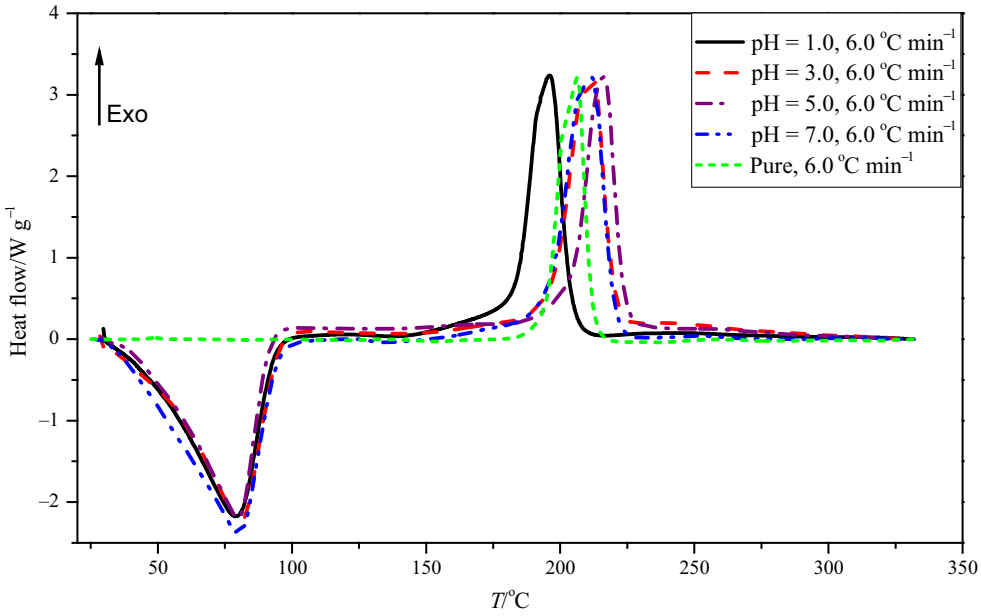

Fig. 5 Heat flow versus temperature curve of DNPT with different pH values by DSC

Table 6 Characteristic parameters for thermal decomposition of DNPT with different pH values by DSC

pH	β/°C min^{-1}	m_{DNPT}/mg	m_{HNO3}/mg	T_0/°C	T_m/°C	T_{end}/°C	$-\Delta H_d$/J g^{-1}
–	6.0	5.0	–	200.0	206.8	208.5	1.10
1	6.0	5.0	5.0	190.2	195.2	199.6	1.39
3	6.0	5.0	5.0	200.2	212.7	214.9	1.28
5	6.0	5.1	5.0	207.5	214.5	216.7	1.35
7	6.0	5.1	5.0	205.4	212.0	214.8	1.46

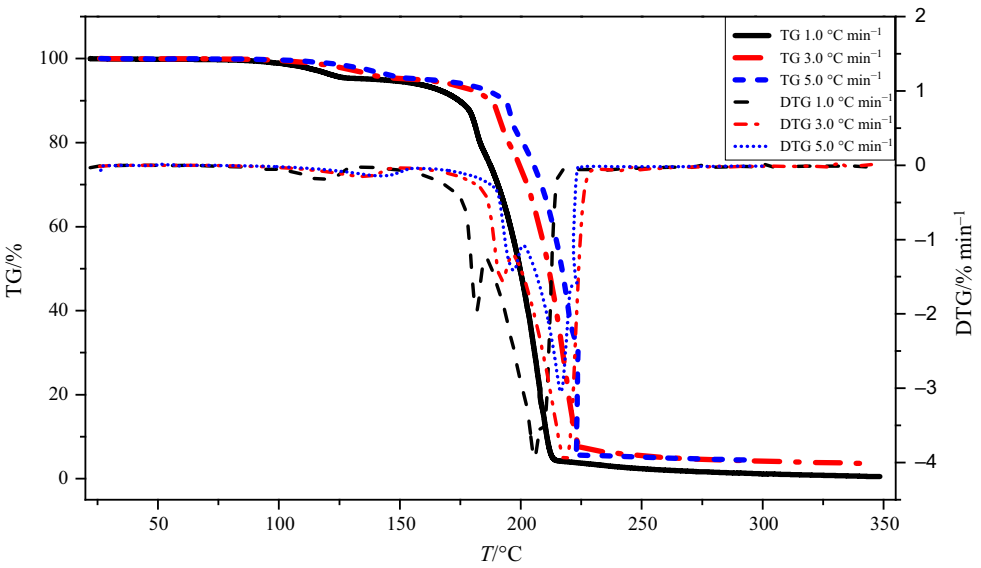

Fig. 6 Thermal curves of DTG and TG for DNPT on various β

The thermal decomposition path of DNPT contributes to understanding the reaction mechanism of DNPT and formulating control measures to forestall thermal runaway of DNPT. According to the DNPT characteristic parameters obtained experimentally, the decomposition path of DNPT could be reasonably predicted by molecular simulation. Gaussian software was adopted to optimize and calculate the groups which were formed after breaking these bonds.

The bond dissociation energy (BDE) is defined as the minimum energy required for chemical bond breakage

Table 7 Characteristic temperature for the decomposition of DNPT by TG

β/°C min^{-1}	Sample mass/mg	T_0/°C	T_m/°C	T_{end}/°C
1.0	19.6	185.3	205.3	216.4
3.0	19.9	196.8	217.9	229.4
5.0	20.1	200.9	217.0	223.8

[21]. The smaller the bond dissociation energy is, the more favorable it is for covalent bonds dissociation. Accordingly, BDE is often used to predict the stability of the covalent bond in compound molecules [22]. At 298 K and 1.01×10^5 Pa, Eqs. (1) and (2) for calculating the BDE of the covalent bond (A–B) in the compound molecules are expressed as follows:

$$BDE_0(A-B) = E_0(A^{\cdot}) + E_0(B^{\cdot}) - E_0(A-B) \quad (1)$$

$$BDE(A-B) = BDE_0(A-B) + \Delta ZPE \quad (2)$$

Figure 8 shows a stable configuration after molecular optimization. Furthermore, the Gaussian software could calculate the single point energies of the optimized DNPT molecules. The single point energy of the DNPT molecule was -1.78×10^6 kJ mol^{-1}. According to Eqs. (1) and (2), the BDEs of all C–N, N–N, and N=O were calculated and compared. Table 8 summarizes the most probable bond dissociation pathways in the pyrolysis process of DNPT, strictly for the energy change at each stage and the dissociation mode on minimum BDE.

In the process of molecular thermal decomposition, the dissociation and generation were concomitant. The free radicals or atoms dissociated in the process of DNPT thermal decomposition would recombine and ultimately generate the reaction products. DNPT thermal

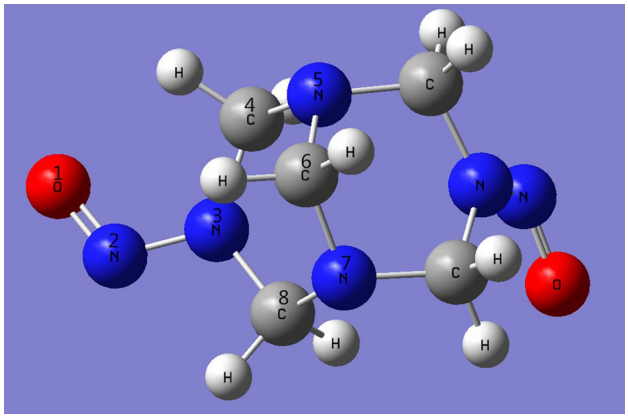

Fig. 8 Stable configurations after molecular optimization

decomposition will generate N_2, HCHO, and $(CH_2)_6N_4$, and the chemical equation of the thermal decomposition is expressed as follows [23]:

$$(CH_2)_5N_4(NO)_2 \longrightarrow \Delta 2N_2 + 2HCHO + \frac{1}{2}(CH_2)_6N_4 \quad (3)$$

In the process of simulation, free radicals or atoms, such as $1M_2$, $4M'_3$, $4M'_2$, $5M_6$, $6M_3$, $7M_1$, and $7M_2$, were generated. The reaction path of DNPT thermal decomposition was predicted, as shown in Fig. 9. N_2 and HCHO were created by the combination $1M_2$, $4M'_3$, $5M_6$ and $7M_2$. $(CH_2)_6N_4$ was generated by the combination of $4M'_2$, $6M_3$, and $7M_1$, which agrees with Eq. (3).

Figure 10 shows the infrared spectra of DNPT when the mass loss rate on the TG-IR experiments was the maximum. Decomposition products of DNPT contained functional groups including aldehydes (C = O, C–H) and tertiary amines (C–N, C–H). This result was beneficial to study the decomposition paths of DNPT by molecular simulation.

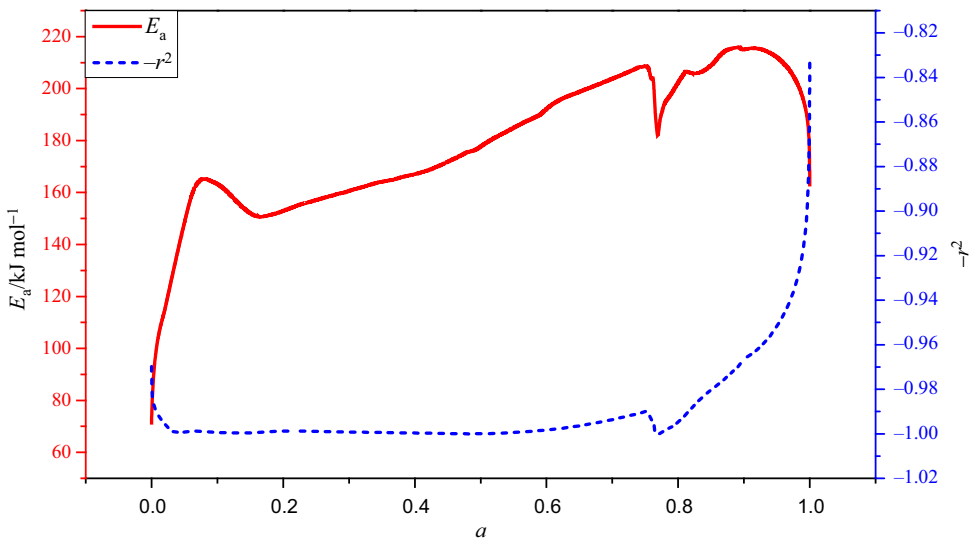

Fig. 7 Curves of the apparent activation energy and the correlation coefficient

Table 8 Energy change and bond decomposition energy during thermal decomposition of DNPT

No.	Group/molecular	Broken covalent bond	ΔE/2627 kJ mol^{-1}	ΔH_d/2627 kJ mol^{-1}	$\Delta E'$/2627 kJ mol^{-1}	*BDE*/2627 kJ mol^{-1}
1	DNPT	$1B_{2,3}$	0.0669	0.0594	0.0107	0.0562
2	$1M_3$	$2B_{3,4}$	129.9927	129.9834	0.00674	129.9860
3	$2M_{3,4}$	$3B_{6,7}$	0.1040	0.0945	0.0120	0.0921
4	$3M_6$	$4M_{6,7}$	0.1236	0.1199	0.0041	0.1195
	$3M_7$	$4B'_{2,3}$	0.1401	0.1344	0.0081	0.1320
5	$4M_{6,7}$	$5B_{5,6}$	0.1085	0.1052	0.0046	0.1039
6	$5M_5$	$6B_{2,3}$	0.1256	0.1171	0.0099	0.1156
7	$6M_2$	$7B_{1,2}$	0.1839	0.1770	0.0095	0.1744

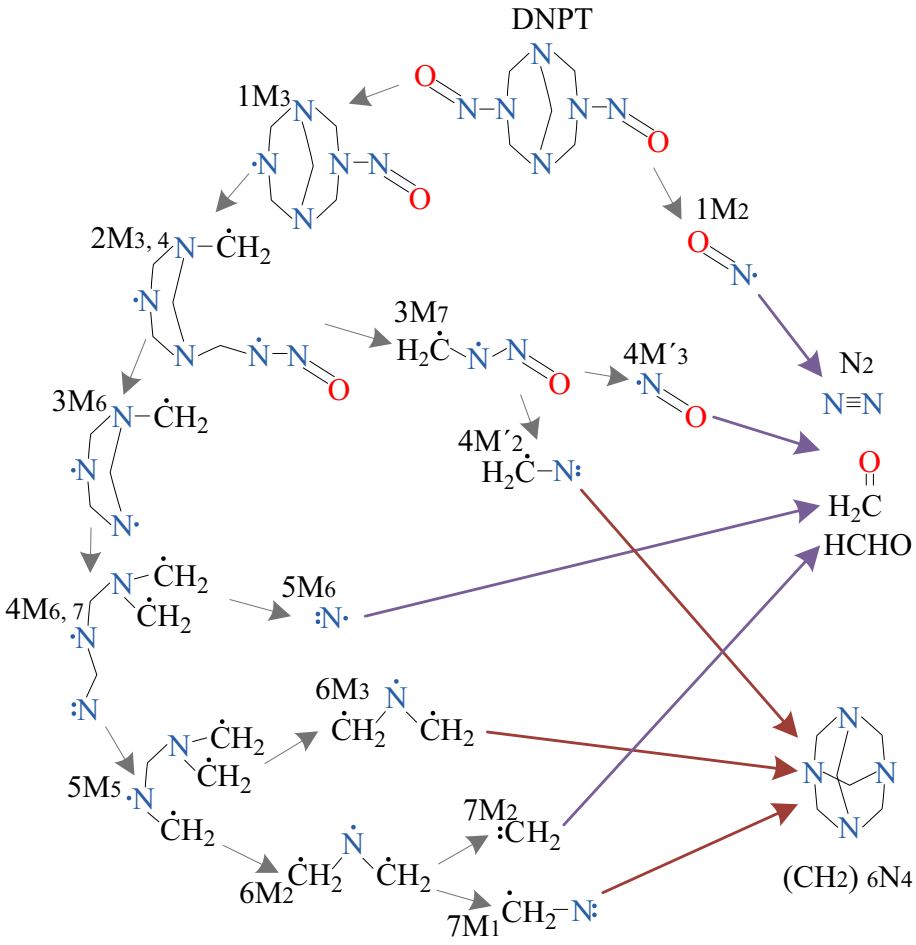

Fig. 9 Schematic diagram of thermal decomposition reaction path of DNPT

Conclusions

In air atmosphere, the exothermic onset temperature of DNPT was 198.6–202.6 °C by DSC experiment, the maximum reaction temperature was 201.5–210.6 °C, and the apparent activation energy of DNPT was 160.83 kJ mol^{-1} by Kissinger method.

The exothermic onset temperature of DNPT was 200.8–206.2 °C in the air when water was added, and the maximum reaction temperature was 201.5–210.6 °C by DSC experiment. T_0, T_m, T_{end}, and ΔH_d all increased when more water was added. The apparent activation energy also increased depending on the amount of water. Water not only reduced the initial temperature of the DNPT reaction, but also increased the reaction intensity. Therefore, dry

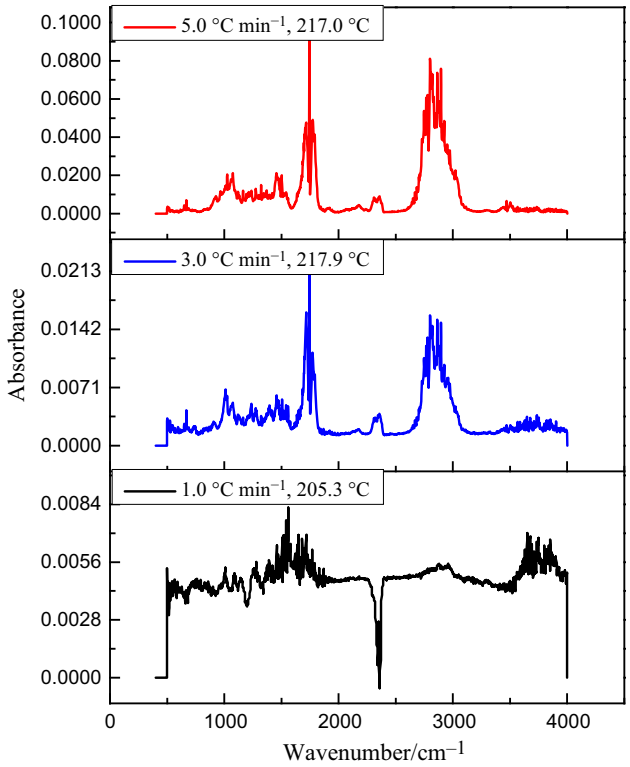

Fig. 10 Infrared spectra of DNPT on maximum mass loss rate in TG experiments

DNPT and the environment are beneficial to the transportation and storage safety of DNPT. In view of property loss prevention and emergency response, adding a large amount of water is inappropriate for reducing the risk of thermal runaway of DNPT.

Inorganic acids did contribute to the reaction of DNPT in air. The effect of water in the solution on the reaction was stronger than that of acid when the pH was larger than or equal to 3. When pH was less than or equal to 1, acid became the decisive factor affecting the reaction. Specific measures should be taken to avoid mixing acids with DNPT.

The exothermic onset temperature of DNPT was 185.3–200.9 °C by TG experiment, and the maximum reaction temperature was 205.3–217.9 °C. The apparent activation energy also fluctuated with respect to α value, and the apparent activation energy of the initial reaction of DNPT was 165.35 kJ mol^{-1}. Considering the safety of hazardous chemicals, the accumulated temperature of DNPT in storage must be below 185 °C. Collision and friction should be avoided during the entire operating process, including transportation and handling.

Infrared spectroscopy experiments were carried out, when the mass loss rate of the reactant was the fastest in TG experiments. According to the infrared spectra results, reaction products contained aldehydes and tertiary amines. HCHO and $(CH_2)_6N_4$ were produced in the thermal decomposition process of DNPT. The most possible dissociation path of DNPT thermal decomposition was found by Gaussian software to simulate decomposition mechanism. The combination of $1M_2$, $4M'_3$, $5M_6$, and $7M_2$ generated N_2 and HCHO. The combination of $4M'_2$, $6M_3$, and $7M_1$ generated $(CH_2)_6N_4$.

Acknowledgements The authors gratefully acknowledge the financial support provided by the National Natural Science Foundation of China (Grant No. 5100-6122) and the National Key Research and Development Program of China (Grant No. 2016-YFC080-1500).

References

1. Chen ZY, Lin HM, Wang L. Study on decomposition temperature of blowing agent. J Zhejiang Inst Sci Technol. 2000;04:7–11.
2. Zhou Y. Study on activation mechanism of merging using blowing agent and its application in natural rubber foaming. Shanghai: Shanghai Jiao Tong University; 2011.
3. Thomson BJ. International co-operation in hazardous materials accident prevention. J Loss Prev Process Ind. 1999;12(3):217–25.
4. Li D. Hangzhou Haihong chemical deflagration event has been in the past year, but the survey report was questioned. Young Times. 2009. http://news.sohu.com/20091121/n268363907.shtml. Accessed 21 Nov 2009.
5. Zhao RW. Cause analysis of "9.2" hazardous chemicals deflagration accident in Shandong, Linyi. Government network of China. http://finance.sina.com.cn/roll/20090910/18483051578.shtml. Accessed 10 Sept 2009.
6. Accident investigation team of "3.26". Taizhou Renhe Chemical Technology Co., Ltd. "3. 26" general deflagration accident investigation report. Safety Supervision Bureau Official Website of Taizhou. http://blog.sina.com.cn/s/blog_724b4a770101ilt4.html. Accessed 20 Jan 2014.
7. Radhakrishnan S, Talawar MB, Venugopalan S, Narasimhan VL. Synthesis, characterization and thermolysis studies on 3, 7-dinitro-1, 3, 5, 7-tetraazabicyclo [3, 3, 1] nonane (DPT): a key precursor in the synthesis of most powerful benchmark energetic materials (RDX/HMX) of today. J Hazard Mater. 2008;152(3):1317–24.
8. Cooney AP, Crampton MR, Scranage JK, Scranage John K. Kinetic studies of the pH dependence of the decomposition of 3, 7-dinitro-1, 3, 5, 7-tetra-azabicyclo [3.3.1] nonane (DPT) and related compounds. J Chem Soc Perk Trans. 1989;2(1):77–81.
9. Liu WJ, Xu ZB, Cui KJ, Xue M. The nitrolysis mechanism of 3, 7-dinitro-1, 3, 5, 7-tetra-azabicyclo [3.3.1] nonane. Propellants Explos Pyrotech. 2015;40(5):645–51.
10. Peng ZL, Zhang YX. Discussion on factors affecting thermal decomposition of foaming agent H. CN Rub Indus. 1995;06:358–62.
11. Peng ZL, Wang J, Zhang XF, Zhang YX. Study on decomposition characteristics of foaming agent H in EPDM composites. CN Rub Indus. 2000;47(8):456–9.
12. Vágenknecht J, Zeman S. Some characteristics of 3,7-dinitro-, 3,7-dinitroso- and dinitrate compounds derived from 1,3,5,7-tetraazabicyclo [3.3.1] nonane. J Hazard Mater. 2005;119(1–3):1–12.
13. Zeman S, Shu Y, Riedl Z, Vágenknecht J. Thermal reactivity of some nitro- and nitroso-compounds derived from 1,3,5,7-tetraazabicyclo [3.3.1] nonane at contamination by ammonium nitrate. J Hazard Mater. 2005;121(1–3):11–21.

14. Zhou Y, Peng ZL, Jiang SQ. Activation mechanism of foaming agent H and its effect on foaming of Natural rubber. CN Rub Indus. 2012;59(7):408–14.
15. Zheng CC, Zhang TZ, Cui ZJ, Han BK, Feng SH. Effect of assistant foaming agent BK and foaming agent H on the foaming properties of NBR/PVC. Spec Purp Rub Prod. 2014;05:30–5.
16. Berlin AA, Shutov FA. Khymiya i tekhnologiya gazonapolnenykh vysokopolymerov (Chemistry and Technology of Foamed High Polymers). Izdat. 1980.
17. Zeman S, Dimun M. Nitrosation cleavage of hexamethylenetetramine in slightly acid media from the aspect of the thermochemistry of the nitrosation agent formation. Thermochim Acta. 1981;51(23):325–34.
18. Zhang MY. Effects of temperature on foaming agent H of emulsified explosive. In: China civilexplosives. Proceedings of CCEIC 6. vol 5; 2004. p. 133–137.
19. Tall A, Zeman S. Determination of heats of decomposition of some 1, 3, 5, 7-tetraazacyclooctane and 1, 3, 5-triazacyclohexane derivatives using differential scanning calorimetry. J Therm Anal Calorim. 1977;12(1):75–81.
20. Stoessel F. Thermal safety of chemical processes. Weinheim: Wiley-VCH; 2008.
21. Lv JY. Study on thermal explosion risk of organic peroxides. Nanjing: Nanjing University of Science and Technology; 2015.
22. Song XS, Yu CR, Linghu RF, Yang XD. Study on the relationship between the dissociation energy of molecular bond and the impact sensitivity of polynitrobenzene. J Atom Mol Phys. 2008;06:1357–61.
23. Wang ZL. Foaming agent and curing system for sponge rubber. Wor Rub Indus. 2008;35(09):7–15.